THE JOURNAL OF BIOLOGICAL CHEMISTRY VOL. 281, NO. 17, pp. 11712–11720, April 28, 2006
Printed in the U.S.A.

# Dissociation of Regulated Trafficking of TRPC3 Channels to the Plasma Membrane from Their Activation by Phospholipase C*[S]

Received for publication, September 26, 2005, and in revised form, January 31, 2006 Published, JBC Papers in Press, March 7, 2006, DOI 10.1074/jbc.M510541200

**Jeremy T. Smyth, Loïc Lemonnier, Guillermo Vazquez, Gary S. Bird, and James W. Putney, Jr.**[1]

*From the Laboratory of Signal Transduction, NIEHS, National Institutes of Health, Department of Health and Human Services, Research Triangle Park, North Carolina 27709*

**Regulated translocation of canonical transient receptor potential (TRPC) proteins to the plasma membrane has been proposed as a mechanism of their activation. By using total internal reflection fluorescence microscopy (TIRFM), we monitored green fluorescent protein-labeled TRPC3 (TRPC3-GFP) movement to the plasma membrane in HEK293 cells stably expressing this fusion protein. We observed no increase in TRPC3-GFP TIRFM in response to the muscarinic receptor agonist methacholine or the synthetic diacylglycerol, 1-oleoyl-2-acetyl-*sn*-glycerol, despite activation of TRPC3 by these agents. We did, however, observe a TIRFM response to epidermal growth factor (EGF). This TIRFM response to EGF was accompanied by increased $Ba^{2+}$ entry and TRPC3 currents. However, 1-oleoyl-2-acetyl-*sn*-glycerol-induced TRPC3 activity was not increased. TIRFM also increased in response to $Gd^{3+}$, a competitive inhibitor of TRPC3 channels. This may be indicative of constitutive trafficking of TRPC3, with $Gd^{3+}$ acting to "trap" cycling TRPC3 molecules in the plasma membrane. Consistent with this interpretation, TRPC3-expressing cells exhibited large variance in membrane capacitance, and this variance was decreased by both $Gd^{3+}$ and EGF. These results indicate the following: (i) trafficking of TRPC3 may play a role in regulating the concentration of channels in the plasma membrane but is not involved in activation through the phospholipase C pathway; (ii) TRPC3 undergoes constitutive cyclical trafficking in the plasma membrane, and the mechanism by which growth factors increase the number of plasma membrane channels may involve stabilizing them in the plasma membrane.**

The mammalian transient receptor potential (TRP)[2] family of cation channel proteins consists of at least 28 members, which have been shown to mediate a wide range of diverse functions, including taste transduction, thermosensation, $Ca^{2+}$ and $Mg^{2+}$ absorption, and $Ca^{2+}$ entry (1–3). Mammalian TRPs have been further divided into three major subgroups as follows: the TRPV group, named after the founding member the vanilloid receptor; the TRPM group, named after the melastatin gene; and the TRPC or canonical TRP group, so named because these proteins share the greatest homology with the original *Drosophila* TRP.

Similarly to *Drosophila* TRP, the TRPC proteins, which consist of seven members (TRPC1–7), are activated downstream of phospholipase C (PLC) (4, 5). PLC is activated as a result of stimulation of G-protein-coupled receptors or receptor protein-tyrosine kinases, and the enzyme is responsible for cleaving its substrate phosphatidylinositol 4,5-bisphosphate ($PIP_2$) into two second messenger molecules, inositol 1,4,5-trisphosphate ($IP_3$) and diacylglycerol (DAG) (6). $IP_3$ induces the release of $Ca^{2+}$ stored within the endoplasmic reticulum by interacting with and gating the $IP_3$ receptor, thus resulting in an increase in the cytoplasmic $Ca^{2+}$ concentration (7). DAG is most recognizable as an activator of protein kinase C (8). The $PIP_2$ hydrolyzing activity of PLC is also an important regulator of TRPC activity, although the mechanisms may differ among TRPC isoforms and depend upon expression conditions and cellular environment. In many cases, TRPC channels can be activated as a consequence of $IP_3$-mediated depletion of intracellular $Ca^{2+}$ stores, *i.e.* they function as capacitative or store-operated calcium channels (9–19). In other instances, TRPC channels appear to be activated as a consequence of PLC activation, but this occurs by a mechanism that does not depend upon store depletion. In this receptor- or PLC-operated mode, the various TRPC isoforms can be grouped into the following two classes based on structural and functional similarities: TRPC3, -6, and -7 are activated by DAG via a protein kinase C-independent mechanism (20–24), and TRPC1, -4, and -5 are activated in some manner subsequent to PLC activation but apparently not by DAG (24, 25).

In addition, there is accumulating evidence that agonist-induced activation of TRPCs may involve their exocytotic insertion into the plasma membrane. Cayouette *et al.* (26) showed by surface biotinylation labeling of HEK293 cells that externalization of overexpressed TRPC6 increases in response to muscarinic receptor stimulation or depletion of intracellular $Ca^{2+}$ stores with thapsigargin. Singh *et al.* (27) also demonstrated carbachol-induced externalization of TRPC3 by surface biotinylation labeling. In both cases channel externalization occurred in the presence of 1,2-bis(2-aminophenoxy)ethane-*N*,*N*,*N*′,*N*′-tetraacetic acid, discounting the possibility of a secondary effect of the $Ca^{2+}$ mobilizing activity of the agonists. Bezzerides *et al.* (28) employed the technique of total internal reflection fluorescence microscopy (TIRFM) together with surface biotinylation to demonstrate transport of overexpressed green fluorescent protein (GFP)-tagged TRPC5 to the plasma membrane in response to treatment with epidermal growth factor (EGF).

An important question regarding directed translocation of TRPC channels to the plasma membrane is whether channel insertion accounts for or to some degree contributes to the mechanism of channel activation by neurotransmitters and hormones. A correlation between translocation of a mammalian TRP with regulation of channel activity was first made by

* This work was supported by the Intramural Program of NIEHS, National Institutes of Health. The costs of publication of this article were defrayed in part by the payment of page charges. This article must therefore be hereby marked "*advertisement*" in accordance with 18 U.S.C. Section 1734 solely to indicate this fact.

[S] The on-line version of this article (available at http://www.jbc.org) contains supplemental movies S1–S3.

[1] To whom correspondence should be addressed: Laboratory of Signal Transduction, NIEHS, National Institutes of Health, Department of Health and Human Services, P. O. Box 12233, Research Triangle Park, NC 27709.

[2] The abbreviations used are: TRP, transient receptor potential; EGF, epidermal growth factor; GFP, green fluorescent protein; OAG, 1-oleoyl-2-acetyl-*sn*-glycerol; $IP_3$, inositol 1,4,5-trisphosphate; DAG, diacylglycerol; $PIP_2$, phosphatidylinositol 4,5-bisphosphate; PLC, phospholipase C; TIRFM, total internal reflection fluorescence microscopy.

Kanzaki *et al.* (29), who showed that insulin-like growth factor I-induced translocation of TRPV2 is responsible for the channel activity that is mediated by the growth factor. The case for a correlation between agonist-induced translocation of TRPC proteins and channel activity has been less clear. In this study we present several new findings that further address the relationship between TRPC translocation and channel activity. First, we have found that under conditions in which agonist-induced TRPC3 activation clearly occurs, TRPC3 translocation to the plasma membrane does not occur. Second, similarly to TRPC5, we have found that TRPC3 translocation to the plasma membrane occurs in response to EGF treatment; however, this increase in surface-expressed TRPC3 channels was not associated with an increase in agonist-induced cation entry. Thus, these results cast doubt on the hypothesis that agonist-induced translocation of TRPC3 to the plasma membrane is necessary for channel activation. Finally, we present evidence that TRPC3 channels undergo constitutive cycling in and out of the plasma membrane, and we suggest that the mechanism of directed trafficking of TRPC3 to the plasma membrane by EGF may involve prevention of re-internalization of these constitutively cycling channels.

## MATERIALS AND METHODS

*Reagents*—Methacholine, thapsigargin, and 1-oleoyl-2-acetyl-*sn*-glycerol (OAG) were purchased from Calbiochem. EGF was from Upstate, and fura-5F and *N*-(3-triethylammoniumpropyl)-4-(4-(dibutylamino) styryl)pyridinium dibromide (FM 1–43) were from Invitrogen. All other chemicals and reagents, unless otherwise specified, were from Sigma.

*TIRF Microscopy*—All experiments were carried out using stable TRPC3-GFP-expressing HEK293 cells (30) maintained in culture as described previously (31). TIRFM was carried out using an Olympus (Melville, NY) IX2-RFAEVA-2 illumination system mounted on an Olympus IX71 inverted microscope. Illumination was provided by a 488-nm argon ion laser (Melles Griot, Carlsbad, CA) directed through a fiber optic cable, and illumination intensity was attenuated as needed by neutral density filters (Chroma Technology Corp., Rockingham, VT). Laser illumination was not toxic to cells, because HEK293 cells loaded with the $Ca^{2+}$ dye Fluo-3 did not exhibit aberrant $Ca^{2+}$ release or signs of degeneration when monitored with this system (data not shown). In TIRFM, incident illumination is angled such that it is totally internally reflected at the interface between the glass coverslip and the aqueous medium that bathes the cells. The angle of the illumination incident on the interface between the glass coverslip and aqueous medium was controlled by adjusting the lateral position of the laser beam prior to passing through a TIRFM 60×, 1.45 N.A. oil immersion objective (Olympus). Thus, TIRF illumination was achieved when the incident angle was greater than the critical angle for the glass ($n$ = 1.518) to aqueous ($n$ = 1.37) interface. The emitted fluorescence passed through a D525/50m filter (Chroma) and was captured by a Photometrics Cascade 512F cooled CCD (Roper Scientific, Tucson, AZ). Acquisition and analysis of images were performed with MetaMorph software (Molecular Devices Corp., Downington, PA). Cells were grown on glass coverslips and were bathed in Hepes-buffered saline solution (HBSS: in mM, 120 NaCl, 5.4 KCl, 1.8 $CaCl_2$, 0.8 $MgCl_2$, 11 glucose, and 20 Hepes, pH 7.4) in a Teflon chamber at room temperature. Prior to the addition of any agonists, cells were first imaged for 3–5 min to establish the base line. For fluorescence intensity analysis, regions of interest were drawn to encompass the visible footprints of individual cells, based on initial bright field images. Data are presented as the ratio of the fluorescence intensity at each time point divided by the fluorescence intensity at the start of the experiment ($F/F_0$), where each value was background-subtracted to correct for the dark-field noise of the camera. Images were captured every 10 s.

*Measurements of $Ca^{2+}$ and $Ba^{2+}$ Entry*—Cells were grown on glass coverslips that were then mounted into Teflon chambers. For fura-5F loading, cells were incubated in Dulbecco's modified Eagle's medium supplemented with 10% heat-inactivated fetal bovine serum, 2 mM glutamine, and 2 $\mu$M fura-5F for 20 min at 37 °C in a humidified 95% air, 5% $CO_2$ incubator. Cells were then washed in HBSS and allowed to equilibrate for at least 10 min at room temperature prior to the start of the experiments. For $Ba^{2+}$ measurements, HBSS was replaced with nominally $Ca^{2+}$-free HBSS, followed by exchange with nominally $Ca^{2+}$-free HBSS supplemented with 2.0 mM $Ba^{2+}$. To measure relative intracellular cation concentrations, excitation illumination was alternated between 340 and 380 nm, and emitted fluorescence was captured at 510 nm under the control of a digital fluorescence imaging system (InCyt Im2, Intracellular Imaging Inc., Cincinnati, OH). Pairs of fluorescence intensity measurements were obtained every 10 s. At the end of each experiment, background fluorescence values at 340 and 380 nm excitation were obtained by exposing the cells to 4 $\mu$M ionomycin and 20 mM $Mn^{2+}$; these values were subtracted from each wavelength measurement for each cell, and data are presented as the ratio of the background-subtracted values for excitation at 340 and 380 nm. Because of the fact that some of these measurements represent a mixture of effects of $Ba^{2+}$ and $Ca^{2+}$ on fura-5F fluorescence, the data were not calibrated to give estimates of intracellular cation concentration. These experiments were performed at room temperature.

*Electrophysiology*—Macroscopic membrane ion currents and capacitance were recorded using the patch clamp technique in its whole-cell configuration. The currents were acquired using pCLAMP-9.2 (Axon Instruments) and analyzed offline using Origin 6 (Microcal) software. The extracellular solution (osmolarity 310 mosM) contained (in mM) NaCl, 145; KCl, 5; Hepes, 10; $MgCl_2$, 1; $CaCl_2$, 2; pH 7.3 (adjusted with NaOH). The intracellular pipette solution (osmolarity 290 mosM/liter) contained (in mM) cesium methanesulfonate, 145; 1,2-bis(2-aminophenoxy)ethane-*N*,*N*,*N*′,*N*′-tetraacetic acid, 10; Hepes, 10; $MgCl_2$, 1; $CaCl_2$, 2.2 (100 nM free $Ca^{2+}$); pH 7.2 (adjusted with CsOH). Patch pipettes were fabricated from borosilicate glass capillaries (WPI Instruments, Waltham, MA). The resistance of the pipettes varied between 3 and 5 megohms. Necessary supplements were added directly to the respective solutions, in concentrations that would not significantly change the osmolarity. Changes in the external solutions were carried out using a multibarrel puffing micropipette with common outflow that was positioned in close proximity to the cell under investigation. During the experiment, the cell was continuously superfused with the solution via a puffing pipette to reduce possible artifacts related to changes between static and moving solutions.

*Surface Biotinylation*—TRPC3-GFP expressing HEK293 cells were grown to ~95% confluency on poly-D-lysine-coated 100-mm plates. Following agonist treatments (performed on-dish in HBSS), cells were washed four times in ice-cold phosphate-buffered saline (PBS: in mM, 137 NaCl, 2.7 KCl, 8.1 $Na_2HPO_4$, 136.1 $KH_2PO_4$, pH 8.0), and then incubated in 1 mg/ml Sulfo-NHS-LC-biotin (Pierce) in PBS for 20 min at 4 °C. Cells were then washed four times in ice-cold PBS containing 100 mM glycine to quench the biotinylation reaction and lysed in lysis buffer (LB: in mM, 50 Tris-HCl, pH 7.5, 150 NaCl, 1 EDTA, 1% v/v Nonidet P-40, 0.25% w/v sodium deoxycholate, 1 phenylmethylsulfonyl fluoride, Complete Mini Protease Inhibitor Mixture Tablet (Roche Applied Science)) for 20 min on ice. Lysates were cleared by centrifugation, and equal amounts of protein were incubated with Neutravidin beads (Pierce) overnight at 4 °C with rotation. The beads were then washed four times in LB and boiled for 5 min in Laemmli sample buffer with 5% $\beta$-mercaptoethanol. Recovered proteins were then analyzed by Western blot as described previously (32). Blots were probed with anti-

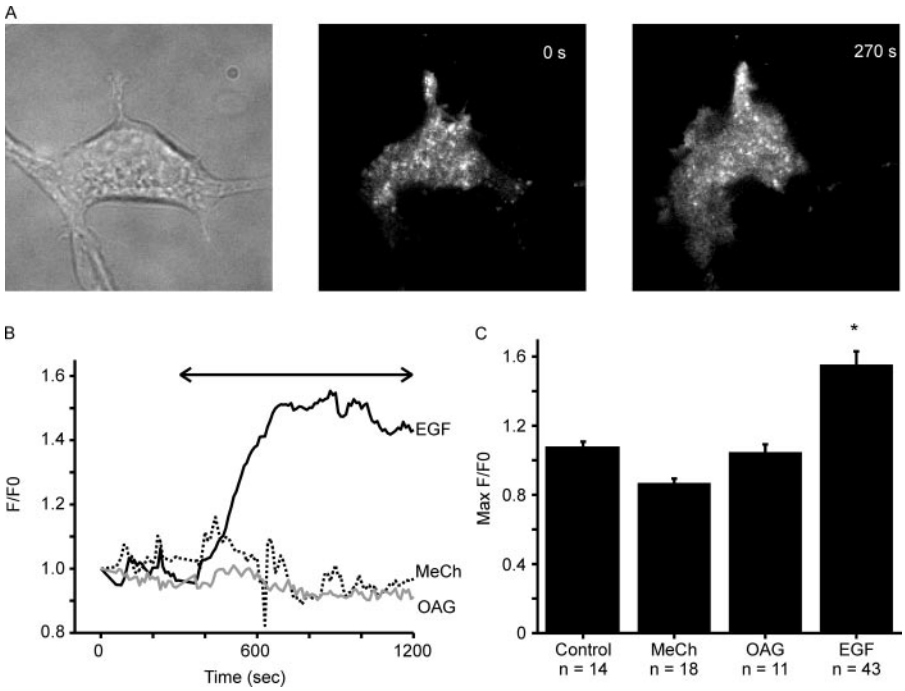


FIGURE 1. **Increase in peripheral TRPC3-GFP fluorescence induced by EGF.** *A,* single TRPC3-GFP-expressing HEK293 cell is shown under bright field illumination (*left panel*), under TIRFM illumination prior to EGF addition (*center panel*), and under TIRFM illumination 270 s following addition of EGF (150 ng/ml). The bright field image was used to delineate the visible footprint of the cell, and this footprint was applied to TIRFM images to define the region of interest that was used for fluorescence intensity measurements. *B,* fluorescence intensity plot corresponding to the EGF-treated cell shown in *A* (*solid black trace*), as well as a cell treated with methacholine (MeCh) (300 $\mu$M; *broken trace*) and a cell treated with OAG (100 $\mu$M; *gray trace*). Background values were subtracted from the individual measurements, and data are plotted as a ratio of each individual measurement to the measurement taken at 0 s. *C,* summarized fluorescence intensity data collected at 15 min following the addition of methacholine (MeCh) (300 $\mu$M), OAG (100 $\mu$M), or EGF (150 ng/ml). Control refers to cells that were exposed to a solution change without the addition of any agonist. A minimum of three coverslips, with 3–8 cells per coverslip, were evaluated; the total number of cells evaluated is indicated *below* each bar. Data are presented as mean ± S.E.; * indicates a statistically significant increase compared with control ($p < 0.05$).

GFP rabbit serum (Invitrogen) to detect TRPC3-GFP. Blots were then stripped and reprobed with anti-pan cadherin polyclonal antibody (AbCam, Cambridge, MA) to normalize for equal amounts of surface-expressed proteins. We confirmed that the biotinylation protocol did not pull down cytoplasmic proteins by reprobing blots with anti-glyceraldehyde-3-phosphate dehydrogenase polyclonal antibody (Santa Cruz Biotechnology). The secondary antibody used for all probings was horseradish peroxidase-conjugated anti rabbit IgG (GE Healthcare, Piscataway, NJ). Band intensities were quantified by densitometry.

*Statistical Analyses*—Comparisons among three or more data groups were made by analysis of variance and between two groups by Student's *t* test. Values of $p < 0.05$ were considered statistically significant.

## RESULTS

*Agonists That Activate TRPC3 Do Not Stimulate TRPC3 Translocation*—The original goal of this project was to determine whether agonists that induce TRPC3 channel activity, such as those that act through $G_q$-coupled receptor pathways, increase trafficking of TRPC3 channels to the plasma membrane and ultimately whether such putative trafficking plays a role in the activation or regulation of channel activity. We utilized TIRFM to monitor, in real time, the dynamics of TRPC3 channels in or near the plasma membrane in HEK293 cells stably expressing TRPC3-GFP. With TIRFM, the evanescent wave of illumination penetrates only ~200 nm into the sample; thus, only fluorophores that are located within 200 nm of the plasma membrane are illuminated and contribute to the TIRFM image (33, 34).

TIRFM images of TRPC3-GFP cells revealed numerous individual punctae of GFP fluorescence, likely indicative of individual TRPC3-GFP-containing structures (see Figs. 1*A* and 7*A* for representative images). Over time, many of these foci of fluorescence disappeared from the image, and new points of fluorescence appeared in different regions of the cell (see supplemental movie), which may be indicative of constitutive trafficking of TRPC3-GFP to and from the plasma membrane (35). Upon treatment of these cells with 300 $\mu$M methacholine, a concentration that resulted in maximal activation of TRPC3 channel activity (30, 31) (data not shown), we failed to observe an increase in the number or intensity of fluorescent punctae in TIRFM images over a time course of 15 min (Fig. 1*B*). Because methacholine activates TRPC3 within seconds following application to cells overexpressing the channel, this result indicates that movement of TRPC3 channels to the plasma membrane is unlikely to be a requisite step in the activation mechanism of TRPC3 channel activity. In agreement with this, we also found that OAG, a membrane-permeant analog of DAG, failed to induce an increase in fluorescence intensity in TIRFM images of TRPC3-GFP cells (Fig. 1*B*). Likewise, depletion of intracellular $Ca^{2+}$ stores with thapsigargin, an inhibitor of the sarco/endoplasmic reticulum $Ca^{2+}$-ATPase, was also without effect (data not shown). Note that in our hands HEK293 cells not transfected with TRPC3 constructs do not respond to PLC-linked agonists or to diacylglycerols under the experimental conditions used in this study (23), ensuring that the $Ca^{2+}$, $Ba^{2+}$, and electrophysiological signals can be attributed to the expressed, GFP-tagged TRPC3 channels that give rise to the TIRFM images.

*EGF Induces Trafficking of TRPC3 Channels to the Plasma Membrane*—Given that translocation of TRPC3 to the plasma membrane does not appear to be required for channel activation by the PLC pathway, we next sought to determine whether increasing the channel concentration by another signaling mechanism can augment TRPC3 activity. Following a recent report by Bezzerides *et al.* (28) showing that EGF causes movement of TRPC5 channels to the plasma membrane, we evaluated the effect of EGF on TRPC3 trafficking. Similarly to its effect on TRPC5 localization, EGF (150 ng/ml) also induced an increase in peripheral TRPC3-GFP localization as evaluated by TIRFM (Fig. 1). In the fluorescence intensity profile shown in Fig. 1*B*, the EGF-induced net movement of TRPC3-GFP to the plasma membrane initiated rapidly and was maximal within 5 min of EGF addition; however, other cells were slower to react, requiring up to 15 min to respond maximally (not shown). On average, an increase of ~50% in peripheral TRPC3-GFP fluorescence was observed 15 min following EGF addition (Fig. 1*C*). To control for possible contributions of changes in cellular or membrane morphology to the TIRFM data, we found that EGF did not induce a significant change in the fluorescence detectable by TIRFM in cells treated with the membrane dye FM 1–43 (data not shown).

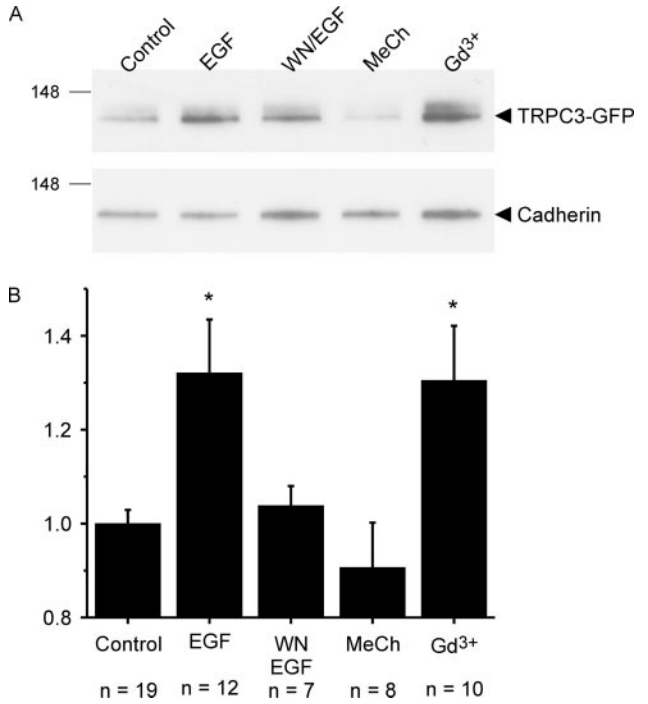


FIGURE 2. **Increase in surface-expressed TRPC3-GFP induced by EGF and $Gd^{3+}$.** *A,* TRPC3-GFP-expressing cells were treated with membrane impermeant biotin and lysed, and biotinylated proteins were precipitated with avidin beads as described under "Materials and Methods." Avidin-precipitated proteins were eluted and analyzed by Western blot using anti-GFP antibody, which recognized a band of ~130 kDa (*upper panel*). The blot was then stripped and reprobed with anti-cadherin antibody, which recognized a band of ~125 kDa (*lower panel*). Prior to biotinylation, cells were either left untreated (control; *1st lane*), treated with EGF (150 ng/ml) for 15 min (*2nd lane*), pretreated with wortmannin (10 nM) for 15 min followed by EGF treatment for 15 min (*3rd lane*), treated with methacholine (100 $\mu$M) for 15 min (*4th lane*), or treated with $Gd^{3+}$ (100 $\mu$M) for 15 min (*5th lane*). *B,* quantification of Western blot band intensities from biotinylation experiments. The intensity of each anti-GFP reactive band, corresponding to TRPC3-GFP, was determined by densitometry, and this value was normalized against the corresponding densitometric value for cadherin. This ratio for each experimental condition was then normalized against the corresponding ratio for the untreated control condition. Data are presented as mean ± S.E.; * indicates a statistically significant increase compared with control ($p < 0.05$).

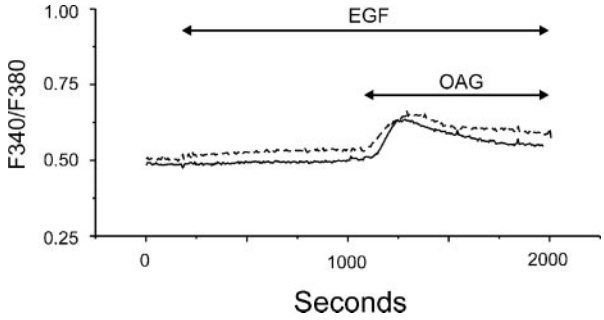


FIGURE 3. **EGF does not augment $Ca^{2+}$ entry.** In the continuous presence of 1.8 mM $Ca^{2+}$ throughout the experiments, cells were either treated with 150 ng/ml EGF for 15 min as indicated by the bar (*broken trace*) or left untreated (*solid trace*), followed by stimulation with 100 $\mu$M OAG. Each trace represents the average of 30 cells on a single coverslip. Results of a single experiment are representative of four.

One caveat of the TIRFM method is that it does not allow one to determine whether a given protein fused to a fluorophore is inserted into the plasma membrane or is merely located in very close proximity to the membrane (*i.e.* within the 200 nm depth of TIRFM illumination). Thus, we performed surface biotinylation studies to determine whether cell surface expression of TRPC3-GFP increases in response to EGF treatment. TRPC3-GFP cells were treated with membrane-impermeant biotin to tag proteins on the cell surface only, and biotin-labeled proteins were then captured with avidin beads. When the avidin-precipitated samples were analyzed by Western blot with an anti-GFP antibody, a band appeared at ~130 kDa, the expected molecular mass of TRPC3-GFP (Fig. 2). More importantly, the intensity of this band significantly increased when cells were treated for 15 min with EGF (150 ng/ml) prior to biotin application, confirming that EGF induces an increase in membrane insertion of TRPC3-GFP. This increase was prevented by pretreatment of cells with 10 nM wortmannin (Fig. 2), an inhibitor of phosphatidylinositol 3-kinase, a result similar to that reported previously for TRPC5 (28). Furthermore, we again failed to detect an increase in surface-expressed TRPC3-GFP in response to treatment of cells with methacholine (Fig. 2) or thapsigargin (data not shown).

*EGF Does Not Increase $[Ca^{2+}]_i$ or Affect the $[Ca^{2+}]_i$ Response to OAG*—Interestingly, the increased number of TRPC3 channels in the plasma membrane induced by EGF did not result in a significant $[Ca^{2+}]_i$ signal (Fig. 3). We expected, as confirmed below with $Ba^{2+}$ entry experiments, that the increase in channels in the plasma membrane would result in a corresponding increase in constitutive TRPC3-mediated cation entry; however, it is likely that the modest increase in constitutively active channels does not produce enough $Ca^{2+}$ entry to overcome plasma membrane and internal $Ca^{2+}$ buffering mechanisms. Furthermore, although EGF is known to activate PLC$\gamma$, we have shown previously that in the absence of serum deprivation EGF does not induce sufficient PLC activity to activate TRPC3 in this cell line (23). Perhaps a more surprising result was that despite an apparent increase in the number of TRPC3 channels, OAG-induced $[Ca^{2+}]_i$ signals were not significantly increased (Fig. 3). As argued below, this may indicate that the additional channels that result from EGF-induced trafficking are not coupled to the machinery necessary for activation by OAG.

*EGF Increases Constitutive TRPC3 Activity Measured as $Ba^{2+}$ Entry or as Membrane Current*—TRPC3-expressing cells generally exhibit significant constitutive activity of plasma membrane TRPC3 channels (30, 36, 37). We were interested in assessing this constitutive activity as an additional indicator of the number of functionally assembled channels in the membrane. Constitutive TRPC3 activity was not observed in fura-based imaging experiments when $Ca^{2+}$ was used as the entrant cation, *i.e.* basal $Ca^{2+}$ was not significantly increased (Fig. 3). However, measurements of changes in $Ca^{2+}$ can be misleading because of the complications from various mechanisms of $Ca^{2+}$ buffering and because of possible effects of membrane potential. Although permeant to TRPC channels, $Ba^{2+}$ is not a substrate of the $Ca^{2+}$ pumps and therefore rapidly accumulates within the cell (38–40). As shown in Fig. 4, TRPC3-GFP-expressing cells exhibited constitutive $Ba^{2+}$ entry that was significantly increased upon pretreatment with 150 ng/ml EGF for 15 min. The 15-min time point was chosen because it was determined in TIRFM experiments that this was the time required for the maximum number of cells to exhibit a significant increase in membrane-localized TRPC3-GFP in response to EGF. No increase in $Ba^{2+}$ entry was observed when $Ba^{2+}$ was added simultaneously with EGF, arguing against more direct effects of EGF through, for example, PLC$\gamma$-induced formation of DAG. The constitutive $Ba^{2+}$ entry is attributable to overexpressed TRPC3 because endogenous cation entry pathways were inhibited in these experiments by the inclusion of 1.0 $\mu$M $Gd^{3+}$ in the extracellular medium (31).

We next carried out whole-cell current measurements to further investigate this effect of EGF treatment on constitutive TRPC3 activity. As shown in Fig. 5*A*, EGF pretreatment (150 ng/ml, 15 min) of TRPC3-GFP-expressing cells augmented both inward and outward TRPC3-mediated basal currents compared with untreated controls. Again, a 15-min EGF pretreatment was required for this effect, because currents

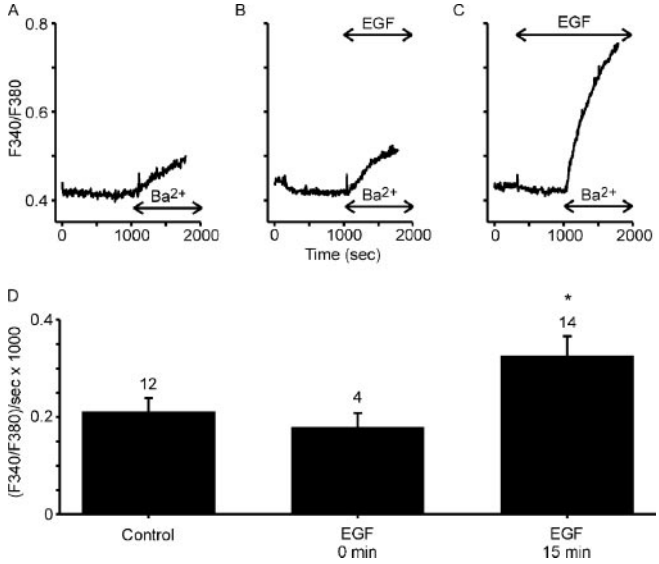


FIGURE 4. **Enhanced TRPC3-mediated constitutive $Ba^{2+}$ entry upon long term EGF treatment.** Representative traces are shown from TRPC3-GFP cells exposed to $Ba^{2+}$ (2.0 mM) in the absence of EGF (*A*), simultaneously with EGF (150 ng/ml) addition (*B*), or 15 min following EGF addition (*C*). Cells were maintained in nominally $Ca^{2+}$-free medium and in the presence of 1.0 $\mu$M $Gd^{3+}$ to inhibit endogenous cation entry. Each trace represents the average response of 30 cells on a single coverslip. *D,* summary data showing the mean rates of $Ba^{2+}$ entry in control cells, cells exposed to $Ba^{2+}$ (2.0 mM) and EGF (150 ng/ml) simultaneously (0 min), and cells exposed to EGF for 15 min prior to $Ba^{2+}$ addition. *Error bars* represent S.E., and the number of coverslips evaluated per condition (with 30 cells per coverslip) is indicated *above* each bar. * indicates a significant increase compared with control ($p < 0.05$).

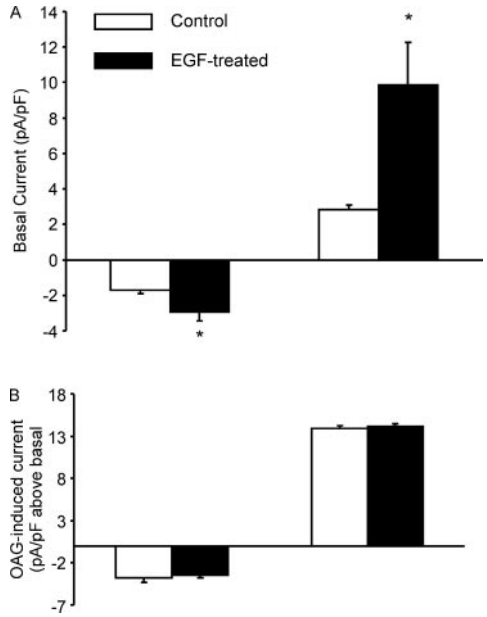


FIGURE 5. **EGF pretreatment increases basal, but not OAG-stimulated, TRPC3-mediated currents.** TRPC3-GFP-expressing HEK293 cells were incubated for 15 min with (*black bars*) or without (*empty bars, control*) 150 ng/ml EGF. After establishing the whole-cell configuration, currents were monitored for up to 3 min under the conditions described under "Materials and Methods." *A,* average outward (+100 mV) and inward (−100 mV) basal TRPC3 whole-cell currents (mean ± S.E.). *B,* after monitoring basal currents, both control (*empty bars*) and EGF-treated (*black bars*) cells were treated with OAG (100 $\mu$M). Average maximal outward (+100 mV) and inward (−100 mV) OAG-stimulated TRPC3 current change (mean ± S.E.) over basal currents are shown.

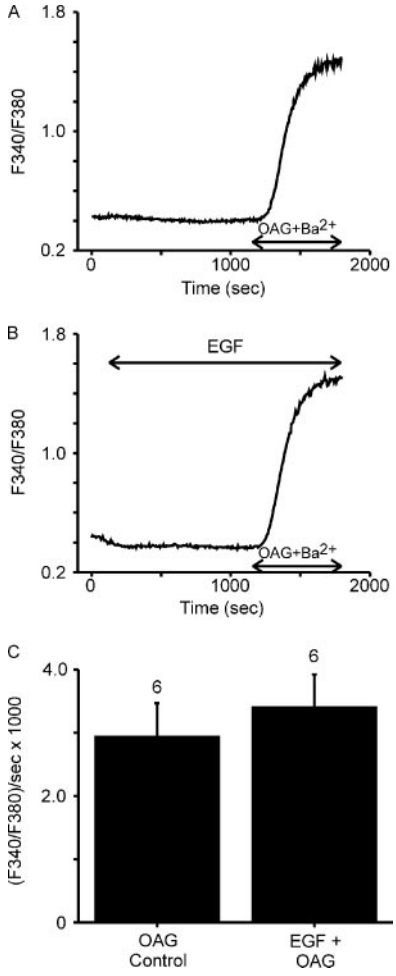


FIGURE 6. **Lack of effect of EGF pretreatment on OAG-induced $Ba^{2+}$ entry.** Representative traces are shown from TRPC3-GFP cells exposed to OAG (100 $\mu$M) and $Ba^{2+}$ (2.0 mM) in the absence of EGF (*A*) or 15 min following EGF (150 ng/ml) addition (*B*). Experiments were performed in nominally $Ca^{2+}$-free medium containing 1.0 $\mu$M $Gd^{3+}$. Each trace represents the average response of 30 cells on a single coverslip. *C,* summary data showing the mean rates of OAG-induced $Ba^{2+}$ entry in control cells and cells pretreated with EGF for 15 min prior to OAG and $Ba^{2+}$ addition. *Error bars* represent S.E., and the number of coverslips evaluated per condition (with 30 cells per coverslip) is indicated *above* each bar.

measured immediately after EGF application were not enhanced compared with controls (data not shown).

*TRPC3 Channels Transported to the Plasma Membrane because of EGF Treatment Cannot Be Activated by OAG*—Next, we further investigated the finding that OAG-activated $Ca^{2+}$ entry was not enhanced following the translocation of channels to the plasma membrane in response to EGF (Fig. 3). Again, to avoid complications from $Ca^{2+}$ buffering or changes in membrane potential, we used $Ba^{2+}$ entry or membrane current as indicators of TRPC3 activity. In cells pretreated with EGF (150 ng/ml, 15 min), $Ba^{2+}$ entry in response to OAG (100 $\mu$M) was not significantly different from that measured in control cells that were not treated with EGF (Fig. 6). We also obtained a similar result when methacholine was used instead of OAG to stimulate TRPC3 activity (data not shown). Again, this result was confirmed with current measurements; the OAG (100 $\mu$M)-induced current was not significantly different in cells pretreated with EGF (150 ng/ml, 15 min) compared with untreated controls (after subtraction of constitutive activity; Fig. 5*B*). Thus, although EGF treatment results in an increase in functional TRPC3 channels in the plasma membrane as evidenced by an increase in constitutive TRPC3 activity, these additional channels appear to be refractory to activation by DAG.

*Increase in TRPC3 Channels in the Plasma Membrane Induced by $Gd^{3+}$*—Low concentrations of $Gd^{3+}$ (~1 $\mu$M) are often included in experiments aimed at evaluating activities of overexpressed TRPC channels because of the ability of $Gd^{3+}$ to inhibit endogenous store-

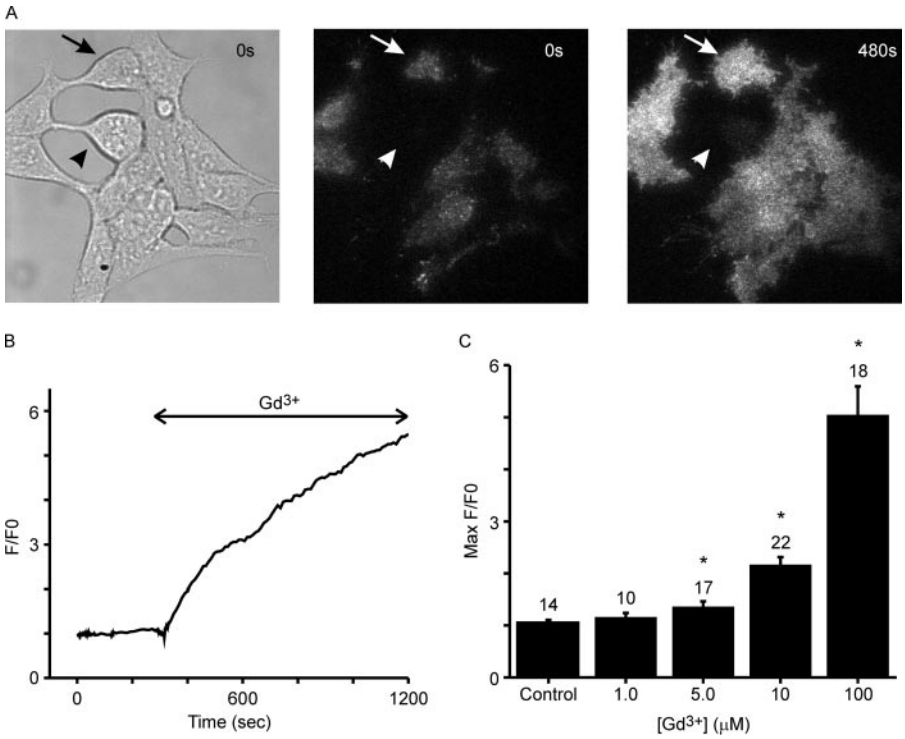


FIGURE 7. **$Gd^{3+}$ induces an increase in peripheral TRPC3-GFP fluorescence.** A bright field image of a field of HEK293 cells expressing TRPC3-GFP (*A, left panel*) was used to define the boundaries of individual cells. A TIRFM image of the same field of cells prior to $Gd^{3+}$ addition is shown in the *center panel*. The *arrow* indicates a cell that exhibited numerous individual foci of fluorescence, likely indicative of individual TRPC3-GFP-containing vesicles. The *arrowhead* indicates a cell that, although clearly visible in the bright field image, did not exhibit any detectable fluorescence in the TIRFM image; it is likely that this cell was not fully attached to the coverslip so as to be within the range of depth of TIRFM illumination, and such cells that were not visible under conditions of TIRFM illumination were not used in further analyses. A TIRFM image taken 480 s after the addition of $Gd^{3+}$ (100 $\mu$M) is shown in the *right panel. B,* fluorescence intensity plot corresponding to a region of interest encompassing the cell defined by the arrow in the *A. C,* summarized fluorescence intensity data collected at 15 min following the addition of a range of $Gd^{3+}$ concentrations from 1 to 100 $\mu$M. Control refers to cells that were exposed to a solution change without the addition of $Gd^{3+}$. A minimum of three coverslips, with 3–8 cells per coverslip, was evaluated per condition; the total number of cells evaluated is indicated *above* each bar. Data are presented as mean ± S.E. * indicates a statistically significant increase above control ($p < 0.05$).

operated $Ca^{2+}$ entry without effect on the activity of the overexpressed channels (31). Higher concentrations (~100 $\mu$M) block TRPC3 channels (37). We investigated the effects of various concentrations of $Gd^{3+}$ to determine whether $Ca^{2+}$ permeation through TRPC3 or endogenous channels plays a role in regulating trafficking. To our surprise, we found that treatment of cells with $Gd^{3+}$ alone was sufficient to induce an increase in peripheral TRPC3-GFP fluorescence as revealed by TIRFM. Cells treated with 100 $\mu$M $Gd^{3+}$, a concentration sufficient to inhibit almost completely TRPC3 channels themselves, exhibited an increase in TRPC3-GFP fluorescence that initiated near the center of the cell footprint and moved radially toward the periphery of the footprint (Fig. 7*A* and supplemental movie). This response initiated rapidly upon $Gd^{3+}$ addition and continued for at least 15 min, although the rate of the fluorescence intensity increase was greatest during the first 5 min following $Gd^{3+}$ addition (Fig. 7*B*). The extent of the increase in TRPC3-GFP fluorescence in response to $Gd^{3+}$ was dependent on the concentration of $Gd^{3+}$ used, with a statistically negligible response at concentrations of 1 $\mu$M and lower (Fig. 7*C*). This concentration dependence is similar to that for binding to and inhibition of the channels by $Gd^{3+}$. Again, we failed to observe a $Gd^{3+}$-induced change in TIRFM fluorescence in FM 1–43-treated cells (data not shown). This does not appear to be a general consequence of blocking permeation through TRPC3 channels, because another TRPC3 blocker, flufenamate (21), did not cause an enhanced TIRF signal (data not shown). We further confirmed that $Gd^{3+}$ induces an increase in surface expression of TRPC3-GFP by surface biotinylation analysis (Fig. 2). We interpret this effect as reflecting the constitutive cycling of TRPC3 channels in and out of the plasma membrane, with $Gd^{3+}$ acting in some manner to prevent re-internalization of the channels. Measurements of membrane capacitance (discussed below) are consistent with this interpretation.

*Whole-cell Capacitance Changes Induced by $Gd^{3+}$ and EGF*—Fusion of vesicles to the plasma membrane can also be measured as an increase in the whole-cell membrane capacitance, because of the increase in the size of the membrane contributed by the vesicle itself (41). As shown in Fig. 8, membrane capacitance in cells overexpressing TRPC3-GFP showed increased fluctuation as compared with wild type cells, again consistent with the idea of constitutive fusion and internalization of vesicles containing TRPC3-GFP. We found that this variability in capacitance rapidly decreased upon treatment of TRPC3-GFP cells with 100 $\mu$M $Gd^{3+}$, although no change was observed upon $Gd^{3+}$ addition to wild type cells. We interpret this decrease in variability as an indication of stabilization of TRPC3-GFP-containing vesicles at the plasma membrane. To the best of our knowledge, such an effect has not been reported previously. We also observed a $Gd^{3+}$-induced increase in the rate of change of capacitance in TRPC3-GFP cells that was not evident in wild type cells. This increase in capacitance over time further supports the idea of a net increase in vesicle fusion in response to $Gd^{3+}$, and the lack of a comparable response in wild type cells implies that fusion of TRPC3-GFP-containing vesicles is responsible for this increase. Finally, although the magnitude of the effects was somewhat smaller, we also observed a decrease in capacitance variability upon treatment of TRPC3-GFP-expressing cells with 150 ng/ml EGF (Fig. 9), as well as a significant increase in the rate of capacitance change upon EGF application, implying incorporation of TRPC3-GFP-containing vesicles into the plasma membrane. The effects of EGF and $Gd^{3+}$ on increasing membrane capacitance and decreasing capacitance variance are not likely secondary to changes in membrane conductance, because EGF increases membrane conductance, and $Gd^{3+}$ is expected to decrease conductance.

## DISCUSSION

*TRPC3 Trafficking Is Not Required for TRPC3 Channel Activation*—Several hypotheses have been developed to explain TRPC channel activation, including stimulation by second messengers such as DAG, conformational coupling of TRPC channels with the $IP_3$ receptor, in some cases involving depletion of $Ca^{2+}$ stores, and secretion-like trafficking of channels to the plasma membrane (4, 5). In this study we have focused on the idea that transport of TRPC3 channels to the membrane is an important aspect of channel activation. In contrast to a previous report by Singh *et al.* (27), we first

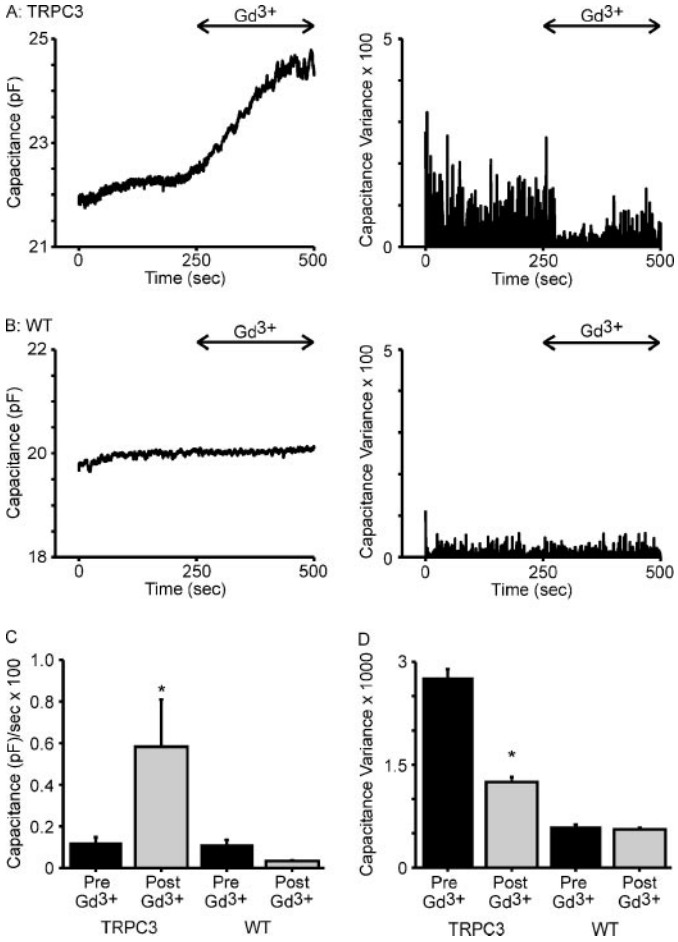


FIGURE 8. **Whole-cell capacitance changes in response to $Gd^{3+}$ treatment.** Membrane capacitance was recorded in the whole-cell configuration in cells stably expressing TRPC3-GFP (*A*) or in wild type cells (*B*). The raw capacitance values are plotted in the *left panels*, and in the *right panels* the variance (defined as the square of the difference between consecutive measurements) of the same capacitance data is plotted. $Gd^{3+}$ (100 $\mu$M) was added in each experiment at 250 s, as indicated by the *arrows*. *C*, the mean rates (±S.E.) of capacitance change are summarized for five TRPC3-GFP-expressing and five wild type (*WT*) cells. The rates were obtained by applying a linear fit to the capacitance data for the 250 s prior to $Gd^{3+}$ addition (pre-$Gd^{3+}$; *black bars*) and 250 s following $Gd^{3+}$ addition (post-$Gd^{3+}$; *gray bars*). *D*, the means (±S.E.) of the capacitance variance data for the 250 s prior to (pre-$Gd^{3+}$; *solid bars*) and 250 s following (post-$Gd^{3+}$; *gray bars*) $Gd^{3+}$ addition for the individual TRPC3-GFP and wild type cells depicted in *A* and *B* are summarized. * indicates a statistically significant change between the pre- and post-conditions in *C* and *D* ($p < 0.05$). This analysis of the change in capacitance variance was performed for each of the five TRPC3-GFP and five wild type cells that were tested, and five of the five TRPC3-GFP cells exhibited a statistically significant decrease in variance in response to $Gd^{3+}$ treatment, whereas only one of the five wild type cells exhibited a significant change ($p < 0.01$).

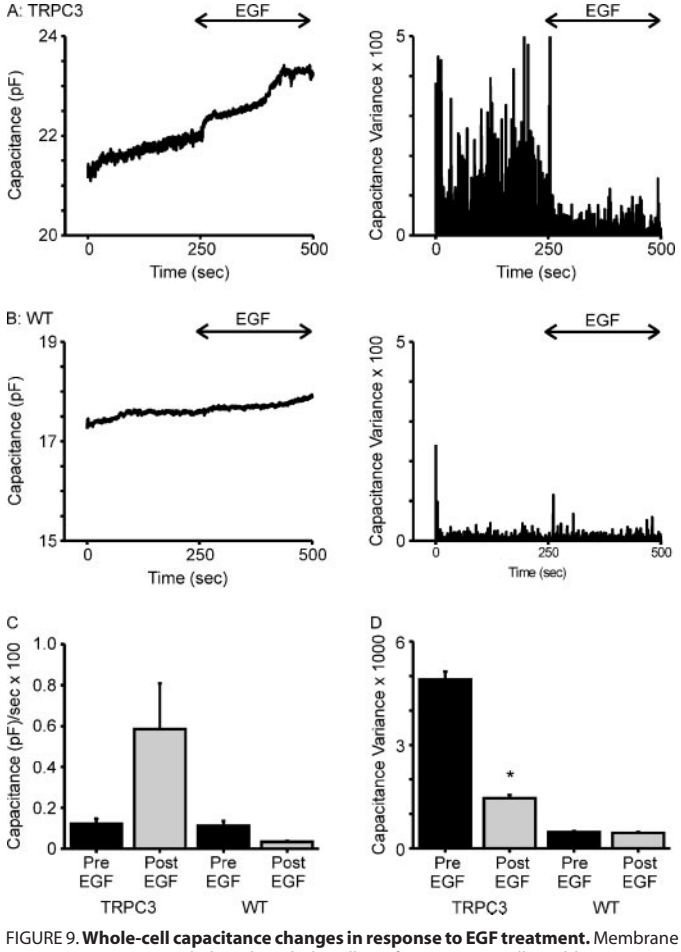


FIGURE 9. **Whole-cell capacitance changes in response to EGF treatment.** Membrane capacitance was recorded in the whole-cell configuration in cells stably expressing TRPC3-GFP (*A*) or in wild type cells (*B*). The raw capacitance values are plotted in the *left panels*, and in the *right panels* the variance (defined as the square of the difference between consecutive measurements) of the same capacitance data is plotted. EGF (150 ng/ml) was added in each experiment at 250 s, as indicated by the *arrows*. *C*, the mean rates (±S.E.) of capacitance change are summarized for four TRPC3-GFP expressing and four wild type (*WT*) cells. The rates were obtained by applying a linear fit to the capacitance data for the 250 s prior to EGF addition (pre-EGF; *black bars*) and 250 s following EGF addition (post-EGF; *gray bars*). *D*, the means (±S.E.) of the capacitance variance data for the 250 s prior to (pre-EGF; *solid bars*) and 250 s following (post-EGF; *gray bars*) EGF addition for the individual TRPC3-GFP, and wild type cells depicted in *A* and *B* are summarized. * indicates a statistically significant change between the pre- and post-conditions in *C* and *D* ($p < 0.05$). This analysis of the change in capacitance variance was performed for each of the four TRPC3-GFP and four wild type cells that were tested, and three of the four TRPC3-GFP cells exhibited a statistically significant decrease in variance in response to EGF treatment, whereas 0 of the four wild type cells exhibited a significant change ($p < 0.05$).

show that neither muscarinic receptor stimulation nor application of the DAG analog, OAG, induced translocation of TRPC3 channels to the plasma membrane, despite robust activation of TRPC3-mediated $Ca^{2+}$ entry under these experimental conditions. A potentially important methodological difference between the Singh *et al.* study (27) and the current study is that Singh *et al.*, using a surface biotinylation assay, observed TRPC3 externalization when cells were stimulated with carbachol at 37 °C, whereas we performed TIRFM and surface biotinylation experiments at room temperature and failed to see externalization. We carried out experiments examining surface biotinylation of TRPC3 at 37 °C; we observed no significant increase in biotinylated TRPC3 in cells treated with methacholine at 37 °C (ratio of methacholine to control: 1.04 ± 0.18, $n = 7$). Furthermore, we did observe TRPC3 externalization following activation of EGF receptors at room temperature, indicating that at room temperature the process of channel trafficking can still occur. Because TRPC3 is readily activated by methacholine at room temperature or at 37 °C, the failure of methacholine to increase externalization indicates that TRPC3 trafficking to the plasma membrane induced by muscarinic receptor stimulation is not a requisite step for TRPC3 activation. Despite this lack of a requirement for translocation, and our failure to observe significant translocation at either temperature, we cannot rule out a limited degree of enhanced trafficking by G-protein-coupled agonists in some situations that may serve to enhance or fine-tune TRPC3 channel activity.

To further test the hypothesis that increasing the number of TRPC3 channels in the plasma membrane augments cation entry mediated by the channel, we were interested to find other agonists that induce trafficking of TRPC3 to the cell surface. In line with the recent report from Bezzerides *et al.* (28), we found that EGF caused an increase in the amount of TRPC3-GFP in the plasma membrane as detected by TIRFM.

Despite the fact that EGF caused significant net movement of TRPC3 channels to the plasma membrane, EGF did not activate a detectable cytoplasmic $Ca^{2+}$ signal; however, EGF did induce small increases in membrane current and rate of entry of $Ba^{2+}$. The magnitude of these changes are as expected for an increase in constitutive activity because of increased channels in the plasma membrane. However, because EGF may induce a slight increase in PLC activity, we cannot rule out partial activation of the TRPC3 channels as well. We also detected changes in the whole-cell capacitance in TRPC3-GFP expressing cells treated with EGF. These changes, namely an increase in the rate of capacitance increase and constitutive channel activity and a decrease in capacitance variability, are consistent with a mechanism involving stabilization of constitutively cycling vesicles at the plasma membrane. Although it is not possible to definitively attribute the capacitance changes to events related to TRPC3-GFP-containing vesicles, the lack of analogous effects in wild type cells implies that overexpressed TRPC3-GFP is responsible. Furthermore, we observed the same patterns of capacitance changes in TRPC3-GFP-expressing cells treated with $Gd^{3+}$, a treatment that also induced a robust increase in the peripheral localization of TRPC3-GFP as detected by TIRFM.

Interestingly, despite a clear increase in plasma membrane TRPC3 channels following EGF treatment, we failed to observe an enhancement of agonist- or OAG-mediated TRPC3 activity. Thus, it appears that the channels that are newly translocated to the membrane in response to EGF are refractory to activation by DAG, at least within the time frame of these experiments. As argued above, the increase in channel number appears to reflect stabilization of constitutively cycling channels in the membrane, rather than introduction of new channels. Thus the insensitivity to DAG activation does not likely reflect qualitative differences in the structure or localization of the additional channels. Possibly, this limit on channel activation results from the fact that we have ectopically expressed TRPC3 in a cell line with limited accessory proteins available for coupling to phospholipase C/diacylglycerol. Thus, regardless of the source of the additional channels, the quantity of these accessory proteins will limit the degree of activation by agonists or diacylglycerol. Nonetheless, this observation further underscores the dissociation between channel trafficking and channel activation. It also provides additional support for our previously stated hypothesis that DAG does not act as a direct regulator of TRPC3 activity but rather requires additional factors (32). Accordingly, we propose that TRPC3 channels that translocate to the plasma membrane in response to treatment with EGF are not activated by DAG because they are not immediately coupled to the putative factor or factors that mediate DAG activation. A similar dissociation between channel translocation and activation was recently demonstrated for TRPC5, because it was shown that TRPC5 translocation induced by bradykinin did not temporally correlate with maximal channel activation conferred by the agonist (42).

*Constitutive Trafficking of TRPC3 Channels*—Our TIRFM and capacitance data support the idea that overexpressed TRPC3 channels constitutively traffic to and from the plasma membrane. The high variance in capacitance we observed in TRPC3-expressing cells and not in wild type cells may be a fortuitous consequence of the degree of expression of channels in these stably transfected cells. In any event, the capacitance fluctuations afford us an additional and independent parameter to aid in understanding the dynamics of TRPC3 trafficking. The effects of $Gd^{3+}$ observed in TIRFM and capacitance experiments can be explained by the ability of $Gd^{3+}$ to bind TRPC3 channels at an external site, resulting in an inability of bound channels to be properly internalized. Thus, $Gd^{3+}$ may essentially "lock" TRPC3-GFP in the plasma membrane, tipping the balance between constitutive exocytosis and endocytosis in favor of the former and leading to rapid accumulation of TRPC3-GFP in the membrane. This alteration of the constitutive trafficking cycle conferred by $Gd^{3+}$ is most evident in the change from a highly variable capacitance to one with less variability, assuming that this variability is indicative of rapid turnover of TRPC3-GFP-containing vesicles at the plasma membrane. Interestingly, EGF also induced a reduction in the variability of the membrane capacitance in TRPC3-GFP cells. This implies that EGF may likewise stabilize TRPC3-GFP in the plasma membrane by preventing its endocytosis, although the mechanism by which EGF accomplishes this is not clear. However, it is becoming increasingly clear that the constitutive cycling of plasma membrane proteins provides a general mechanism for regulation of surface membrane proteins (35).

Recent reports from several laboratories have begun to unravel the processes that regulate TRPC protein localization. As with many signaling molecules that act in a membrane-delimited fashion, it has been demonstrated that TRPC3 interacts with caveolin-1, a marker for caveolae (43), and disruption of the actin cytoskeleton disrupts localization of caveolin-1 and TRPC3 at the plasma membrane (43), as well as TRPC3-mediated cation entry (43, 44). Furthermore, it was shown that members of the soluble *N*-ethylmaleimide-sensitive factor attachment protein receptor (SNARE) complex, which are involved in vesicle docking and fusion with the plasma membrane, regulate localization of TRPC3 at the plasma membrane (27). However, on the basis of our finding that TRPC3 undergoes constant constitutive cycling, it is difficult to assess whether the interaction of TRPC3 with SNARE proteins and the diminution of TRPC3 activity upon cytoskeleton disruption reflect effects on constitutive trafficking of TRPC3 to the plasma membrane or regulated translocation events. In the case of TRPC5, it was shown that activation by EGF of phosphatidylinositol 3-kinase, with subsequent activation of phosphatidylinositol 5-kinase via the small GTPase Rac1, is responsible for translocation of the channel. Thus, by virtue of the ability of phosphatidylinositol 5-kinase to generate $PIP_2$, an increase in $PIP_2$ levels in the plasma membrane may serve to recruit TRPC5 channels to the cell surface (28). We also found that externalization of TRPC3-GFP is sensitive to inhibition by low concentrations of wortmannin sufficient to inhibit phosphatidylinositol 3-kinase; however, an exhaustive analysis of this signaling pathway in the regulation of TRPC3 trafficking was outside the scope of this current study. Finally, it has recently been reported that TRPC3 couples with PLC$\gamma$ to form a functional pleckstrin homology domain that binds $PIP_2$ and is required for the proper localization of TRPC3 in the plasma membrane (45).

In conclusion, we have provided evidence that translocation of TRPC3 protein to the plasma membrane is regulated through receptors for the growth factor, EGF, but not through G-protein-coupled muscarinic receptors or the PLC-derived messenger DAG. Thus, regulation of channel trafficking is not obligatory for channel activation, and in fact, newly translocated channels may be uncoupled from activation by the G-protein PLC pathway. This latter observation supports our previously published contention that TRPC3 is not activated by a direct interaction with DAG. Thus, directed translocation of TRPC3 channels may be a mechanism by which cells can fine-tune $Ca^{2+}$ entry events, but this clearly is not a critical step leading to channel activation. Finally, we provide evidence that TRPC3 channels undergo constant cycling in and out of the plasma membrane and that the mechanism by which growth factors increase the amount of channels in the plasma membrane might be by stabilizing the channels and preventing their reinternalization.

*Acknowledgments—We are grateful for comments and criticisms from Christian Erxleben and David Miller.*

## REFERENCES


1. Clapham, D. E., Runnels, L. W., and Strubing, C. (2001) *Nat. Rev. Neurosci.* **2,** 387–396
2. Montell, C. (2001) *Science's STKE* http://stke.Sciencemag.org/cgi/content/full/sigtrans;2001/90/re1
3. Wissenbach, U., Niemeyer, B. A., and Flockerzi, V. (2004) *Biol. Cell* **96,** 47–54
4. Putney, J. W., Jr. (2004) *Trends Cell Biol.* **14,** 282–286
5. Vazquez, G., Wedel, B. J., Aziz, O., Trebak, M., and Putney, J. W., Jr. (2004) *Biochim. Biophys. Acta* **1742,** 21–36
6. Rhee, S. G. (2001) *Annu. Rev. Biochem.* **70,** 281–312
7. Berridge, M. J. (1993) *Nature* **361,** 315–325
8. Newton, A. C. (2002) *Methods Enzymol.* **345,** 499–506
9. Freichel, M., Suh, S. H., Pfeifer, A., Schweig, U., Trost, C., Weissgerber, P., Biel, M., Philipp, S., Freise, D., Droogmans, G., Hofmann, F., Flockerzi, V., and Nilius, B. (2001) *Nat. Cell Biol.* **3,** 121–127
10. Zitt, C., Zobel, A., Obukhov, A. G., Harteneck, C., Kalkbrenner, F., Lückhoff, A., and Schultz, G. (1996) *Neuron* **16,** 1189–1196
11. Philipp, S., Hambrecht, J., Braslavski, L., Schroth, G., Freichel, M., Murakami, M., Cavalié, A., and Flockerzi, V. (1998) *EMBO J.* **17,** 4274–4282
12. Philipp, S., Cavalié, A., Freichel, M., Wissenbach, U., Zimmer, S., Trost, C., Marguart, A., Murakami, M., and Flockerzi, V. (1996) *EMBO J.* **15,** 6166–6171
13. Vazquez, G., Wedel, B. J., Trebak, M., Bird, G. St. J., and Putney, J. W., Jr. (2003) *J. Biol. Chem.* **278,** 21649–21654
14. Vazquez, G., Lièvremont, J.-P., Bird, G. St. J., and Putney, J. W., Jr. (2001) *Proc. Natl. Acad. Sci. U. S. A.* **98,** 11777–11782
15. Liu, X., Wang, W., Singh, B. B., Lockwich, T., Jadlowiec, J., O'Connell, B., Wellner, R., Zhu, M. X., and Ambudkar, I. S. (2000) *J. Biol. Chem.* **275,** 3403–3411
16. Lievremont, J. P., Bird, G. S., and Putney, J. W., Jr. (2004) *Am. J. Physiol.* **287,** C1709–C1716
17. Mori, Y., Wakamori, M., Miyakawa, T., Hermosura, M., Hara, Y., Nishida, M., Hirose, K., Mizushima, A., Kurosaki, M., Mori, E., Gotoh, K., Okada, T., Fleig, A., Penner, R., Iino, M., and Kurosaki, T. (2002) *J. Exp. Med.* **195,** 673–681
18. Zeng, F., Xu, S. Z., Jackson, P. K., McHugh, D., Kumar, B., Fountain, S. J., and Beech, D. J. (2004) *J. Physiol.* (*Lond.*) **559,** 739–750
19. Yildirim, E., Kawasaki, B. T., and Birnbaumer, L. (2005) *Proc. Natl. Acad. Sci. U. S. A.* **102,** 3307–3311
20. Hofmann, T., Obukhov, A. G., Schaefer, M., Harteneck, C., Gudermann, T., and Schultz, G. (1999) *Nature* **397,** 259–262
21. Inoue, R., Okada, T., Onoue, H., Hara, Y., Shimizu, S., Naitoh, S., Ito, Y., and Mori, Y. (2001) *Circ. Res.* **88,** 325–332
22. Okada, T., Inoue, R., Yamazaki, K., Maeda, A., Kurosaki, T., Yamakuni, T., Tanaka, I., Shimizu, S., Ikenaka, K., Imoto, K., and Mori, Y. (1999) *J. Biol. Chem.* **274,** 27359–27370
23. Trebak, M., Bird, G. St. J., McKay, R. R., Birnbaumer, L., and Putney, J. W., Jr. (2003) *J. Biol. Chem.* **278,** 16244–16252
24. Venkatachalam, K., Zheng, F., and Gill, D. L. (2003) *J. Biol. Chem.* **278,** 29031–29040
25. Schaefer, M., Plant, T. D., Obukhov, A. G., Hofmann, T., Gudermann, T., and Schultz, G. (2000) *J. Biol. Chem.* **275,** 17517–17526
26. Cayouette, S., Lussier, M. P., Mathieu, E. L., Bousquet, S. M., and Boulay, G. (2004) *J. Biol. Chem.* **279,** 7241–7246
27. Singh, B. B., Lockwich, T. P., Bandyopadhyay, B. C., Liu, X., Bollimuntha, S., Brazer, S. C., Combs, C., Das, S., Leenders, A. G., Sheng, Z. H., Knepper, M. A., Ambudkar, S. V., and Ambudkar, I. S. (2004) *Mol. Cell* **15,** 635–646
28. Bezzerides, V. J., Ramsey, I. S., Kotecha, S., Greka, A., and Clapham, D. E. (2004) *Nat. Cell Biol.* **6,** 709–720
29. Kanzaki, M., Zhang, Y.-Q., Mashima, H., Li, L., Shibata, H., and Kojima, I. (1999) *Nat. Cell Biol.* **1,** 165–170
30. McKay, R. R., Szmeczek-Seay, C. L., Lièvremont, J.-P., Bird, G. St. J., Zitt, C., Jüngling, E., Lückhoff, A., and Putney, J. W., Jr. (2000) *Biochem. J.* **351,** 735–746
31. Trebak, M., Bird, G. St. J., McKay, R. R., and Putney, J. W., Jr. (2002) *J. Biol. Chem.* **277,** 21617–21623
32. Vazquez, G., Wedel, B. J., Kawasaki, B. T., Bird, G. S., and Putney, J. W., Jr. (2004) *J. Biol. Chem.* **279,** 40521–40528
33. Axelrod, D. (2001) *Traffic* **2,** 764–774
34. Steyer, J. A., and Almers, W. (2001) *Nat. Rev. Mol. Cell Biol.* **2,** 268–275
35. Royle, S. J., and Murrell-Lagnado, R. D. (2003) *BioEssays* **25,** 39–46
36. Zitt, C., Obukhov, A. G., Strübing, C., Zobel, A., Kalkbrenner, F., Lückhoff, A., and Schultz, G. (1997) *J. Cell Biol.* **138,** 1333–1341
37. Zhu, X., Jiang, M., and Birnbaumer, L. (1998) *J. Biol. Chem.* **273,** 133–142
38. Kwan, C. Y., and Putney, J. W., Jr. (1990) *J. Biol. Chem.* **265,** 678–684
39. Kreye, V. A., Hofmann, F., and Muhleisen, M. (1986) *Pfluegers Arch.* **406,** 308–311
40. Uvelius, B., Sigurdson, S. B., and Johansson, B. (1974) *Blood Vessels* **11,** 245–259
41. von Gersdorff, H., and Matthews, G. (1999) *Annu. Rev. Physiol.* **61,** 725–752
42. Ordaz, B., Tang, J., Xiao, R., Salgado, A., Sampieri, A., Zhu, M. X., and Vaca, L. (2005) *J. Biol. Chem.* **280,** 30788–30796
43. Lockwich, T., Singh, B. B., Liu, X., and Ambudkar, I. S. (2001) *J. Biol. Chem.* **276,** 42401–42408
44. Ma, H.-T., Patterson, R. L., van Rossum, D. B., Birnbaumer, L., Mikoshiba, K., and Gill, D. L. (2000) *Science* **287,** 1647–1651
45. van Rossum, D. B., Patterson, R. L., Sharma, S., Barrow, R. K., Kornberg, M., Gill, D. L., and Snyder, S. H. (2005) *Nature* **434,** 99–104